Proceedings of the Institution of Mechanical Engineers, Part B: Journal of Engineering Manufacture

Fracture Toughness of a Zirconia Engineering Ceramic and the Effects Thereon of Surface Processing with Fibre Laser Radiation

P P Shukla, J Lawrence and H Wu

The online version of this article can be found at:

Published by:

$SAGE

On behalf of:

Institution of MECHANICAL ENGINEERS

Institution of Mechanical Engineers

Additional services and information for *Proceedings of the Institution of Mechanical Engineers, Part B: Journal of Engineering Manufacture* can be found at:

Email Alerts: http://pib.sagepub.com/cgi/alerts

Subscriptions: http://pib.sagepub.com/subscriptions

Reprints: http://www.sagepub.com/journalsReprints.nav

Permissions: http://www.sagepub.com/journalsPermissions.nav

Citations: http://pib.sagepub.com/content/224/10/1555.refs.html

>> Version of Record - Oct 1, 2010

What is This?

Fracture toughness of a zirconia engineering ceramic and the effects thereon of surface processing with fibre laser radiation

P P Shukla[1]*, **J Lawrence**[1], and **H Wu**[2]
[1]Wolfson School of Mechanical and Manufacturing Engineering, Loughborough University, Loughborough, UK
[2]Department of Materials, Loughborough University, Loughborough, UK

Abstract: Vickers hardness indentation tests were employed to investigate the near-surface changes in the hardness of a fibre laser-treated and an as-received ZrO_2 engineering ceramic. Indents were created using 5, 20, and 30 kg loads to obtain the hardness. Optical microscopy, white-light interferometry, and a coordinate measuring machine were then used to observe the crack lengths and crack geometry. Palmqvist and half-penny median crack profiles were found, which dictated the selection of the group of equations used herein. Computational and analytical approaches were then adapted to determine the K_{1c} of ZrO_2. It was found that the best applicable equation was: $K_{1c} = 0.016\,(E/H)^{1/2}\,(P/c^{3/2})$, which was confirmed to be 42 per cent accurate in producing K_{1c} values within the range of 8 to 12 MPa m$^{1/2}$ for ZrO_2. Fibre laser surface treatment reduced the surface hardness and produced smaller crack lengths in comparison with the as-received surface. The surface crack lengths, hardness, and indentation loads were found to be important, particularly the crack length, which significantly influenced the end K_{1c} value when $K_{1c} = 0.016\,(E/H)^{1/2}\,(P/c^{3/2})$ was used. This is because, the longer the crack lengths, the lower the ceramic's resistance to indentation. This, in turn, increased the end K_{1c} value. Also, the hardness influences the K_{1c}, and a softer surface was produced by the fibre laser treatment; this resulted in higher resistance to crack propagation and enhanced the ceramic's K_{1c}. Increasing the indentation load also varied the end K_{1c} value, as higher indentation loads resulted in a bigger diamond footprint, and the ceramic exhibited longer crack lengths.

Keywords: fracture toughness (K_{1c}), Vickers indentation technique, ZrO_2 engineering ceramics

1 INTRODUCTION

Applications of ceramics have been limited owing to their crack sensitivity and low fracture toughness (K_{1c}). Nevertheless, the use of ceramics has increased over the years. They are now considered to be new-age materials, used to manufacture components for the aerospace, automotive, military, and power-generation sectors. Engineering ceramics offer exceptional mechanical properties, which allows them to replace the more conventional materials currently used for high-demanding applications. The engineering applications of various advanced ceramics have been amply demonstrated [1–7]. The Vickers indentation method, applicable for calculating the K_{1c} of the Si_3N_4 ceramic, has been employed by Shukla [8] using the methodology derived by Ponton and Rawlings [9, 10]. McColm identified various indentation techniques to determine the hardness of a variety of ceramics [11]. Strengthening of ceramics through dislocation generation by various mechanical means was conducted by Mitcjell [12], Castaing and Mazumder [13] and Rabier [14]. CO_2 laser treatment of Si_3N_4 ceramics in particular was presented in the work of Mohanty and Mazumder [15], showing enhancement of the flexural strength of the tested ceramic. Ahn et al. [16] used the

Corresponding author: Optical Engineering, Wolfson School of Mechanical and Manufacturing Engineering, Loughborough University, Loughborough LE11 3TU, UK.
email: pratik.shukla@talk21.com

indentation method to investigate the residual stresses in machined ceramics using an X-ray diffraction technique. Several other investigations also used various indentation methods for determining the K_{1c} of hard, brittle materials, using empirical equations applicable for radial median and Palmqvist crack systems, as well as the influence of the ceramic's grain size on the K_{1c} and elastic/plastic damage from the indentation method [17–38]. The British standard (ISO 6507-1) [39] demonstrates the techniques that are required to be complied with during the Vickers indentation tests. Complying with the regulations ensured that the tests conducted on the ceramics were valid. Moreover, other investigators further demonstrated the use of a more empirical equation, further illustrated in this paper, and the accuracy and validation of the equation, as well as the machine accuracy of various indentation techniques [40–48].

The K_{1c} is a very important property of any material. This is especially so for ceramics, owing to their brittle nature. Materials with high K_{1c} are much softer and more ductile. Those types of material can resist cracks at relatively higher stress levels and loading [9–13]. Materials with low K_{1c}, such as most ceramics, are much harder and more brittle and allow crack propagation at lower stresses and loading. Unlike with metals, it is difficult for dislocations to propagate with ceramics, which makes them brittle [14–16]. Ceramics also do not yield mechanically as well as metals, which leads to a much lower resistance to fracture. Ceramics, in comparison with metals and metal alloys, have a low K_{1c}; thus, it would be an advantage if the K_{1c} of ceramics could be improved. This could open new avenues for ceramics to be applicable in high-demanding applications where metals and metal alloys fail owing to their relatively low thermal resistance, coefficient of friction, wear rate, and hardness. This study investigated the use of empirical equations from the literature to calculate the K_{1c} of a ZrO_2 engineering ceramic and observed the effects thereon of fibre laser radiation to effect surface treatment.

In comparison with a CO_2 laser, the fibre laser has a much shorter wavelength, and so it would be interesting to investigate further the effect of short-wavelength radiation on the surface properties of a ZrO_2 engineering ceramic. In addition, although the Nd:YAG laser wavelength is in the same region as that of the fibre laser, the Nd:YAG laser cannot be operated stably in the continuous-wave (CW) mode, which is required to minimize the thermal shock induced in a ceramic. As one can see, this work is timely, as minimal research has been conducted into employing fibre lasers for the surface treatment of materials, particularly engineering ceramics.

K_{1c} is a measure of a material's resistance to fracture or crack propagation. It is the plane strain fracture toughness. Materials with high K_{1c} are much softer and more ductile. Those types of material are resistant to crack generation when exposed to high stresses and loading. The measurement of K_{1c} was carried out using the Vickers indentation method, which calibrates the hardness of the material and induces a crack. The measured hardness and crack lengths were then placed into empirical equations to calculate the material's K_{1c} after and prior to the fibre laser surface treatment. The K_{1c} of engineering materials can be determined using various different techniques.

2 BACKGROUND TO DETERMINE THE K_{1c} OF CERAMICS

2.1 Vickers indentation technique

Single-edge notched beam (SENB), chevron notched beam (CVNB), and double-cantilever beam (DCB), as well as the Vickers indentation method, are all conventionally employed for industrial applications. The Vickers indentation test can be used to determine the K_{1c} of ceramics and glasses from empirical relationships, as demonstrated in references [8] to [17]. Advantages of the Vickers hardness test are the cost-effectiveness and ease of set-up, and it is one of the simplest and least time-consuming in comparison with the other techniques available to determine the K_{1c} of ceramics. The Vickers indentation test method is less responsive in comparison with other techniques, but minimum preparation is required, with quick and cost-effective set-up and use. There are disadvantages to the Vickers indentation test, such as the lack of accuracy to measure the length of the cracks, which influences the final K_{1c} value [9, 10], the diversity of the use of the indentation equations, and its accuracy. The crack lengths are visualized after the test has been conducted by means of optical microscopy. Change in the K_{1c} has an influence on the material's functionality or the diversity of its applications. Improving the K_{1c} of a material can enhance its functional capabilities, such as longer functional life or improved performance under higher cyclic and mechanical loading, particularly for demanding applications where engineering ceramics are applicable. This paper illustrates a method to determine the K_{1c} by using the Vickers indentation method for the laser-treated, cold isostatic pressed (CIP) ZrO_2 ceramics. The test samples were investigated for their near surface hardness, generated crack profiles, and the surface finish, from the diamond indentations prior to and after the laser treatment.

K_{1c} can be determined using the Vickers indentation technique, which measures the hardness of the material by punching an indentation, with the aid of a diamond indenter, to produce a crack in the

material surface [9, 10, 18]. Measured hardness and the crack lengths are then placed into an empirical equation to calculate the material's K_{1c} [9–13, 19]. The results from the Vickers indentation test can then be applicable to the empirical equations that were derived by Ponton [9, 10], Chicot [18], and Liang et al. [20]. The equations derived by Ponton et al. [9, 10] originate from various other authors [21–31]. However, they are modified and applied specifically to hard and brittle materials, such as ceramics and glass [9, 10]. The equations have a geometrical relationship with various ceramics. Different ceramics have various equations applicable to calculate their K_{1c}. Preparation of the samples involves polishing in order to create a reflective surface plane (this would mean that the surface has been well polished) [9, 10, 32, 33] prior to the Vickers indentation process. There are still constraints with the Vickers indentation techniques, as reported by Gong [34], compared with the more conventional techniques applied, such as the SENB and double-torsion (DT) methods, as mentioned elsewhere [17, 35–37]. The constraints are: (a) the dependence of the crack geometry on the applied indentation load and the properties of the material; (b) indentation deformation (non-uniform fracture progression or rapid fracture growth), such as lateral cracking; and (c) unsuitable consideration of the effect of Young's modulus and the material hardness [17].

The procedure and steps necessary to produce a genuine Vickers indentation test result and genuinely valid K_{1c} values are:

1. Each indentation must be performed at a sufficient distance from another. This will prevent the formed cracks interconnecting and bridging with the other diamond indentations created on the ceramic surface [38, 39].
2. A minimum load of 50 N must be used and is recommended because the ceramic materials are of sufficient hardness to require enough loading to produce an indentation.
3. It is ideal to coat the test surface with gold so that the performed indentations are visible. Post-indentation coating may affect the crack tip and give an inaccurate reading.
4. The test samples should be near to $20c$ in thickness and have minimum porosity. The author also stated that the adjacent indentations should be no closer than $4c$.

3 PROPAGATION OF THE CRACK GEOMETRY DURING THE VICKERS INDENTATION TEST

Liang et al. [20] followed an investigation into the K_{1c} of ceramics using the indentation method. He also used several equations by various authors, as listed in reference [20]. It was stated by Liang et al. that equations differ as the crack geometry changes (from Palmqvist to median half-penny cracks). He introduced a new equation, stated elsewhere [20], which was said to be more universal than previous work. However, in order for the formula to be used, it had to be manipulated sufficiently. Ponton and Rawling's [9, 10] formula, in comparison, was much simplified and was easy to apply. Chicot [18] conducted further investigation by applying two other equations to produce results using materials such as tungsten carbide (nickel phosphorus-treated) and pure silicon. He used the concept of a median half-penny crack and a Palmqvist crack system to determine the most applicable equation [18]. It was stated that high indenter loads produce a median half-penny crack within the material that is on the edges of the diamond indentation (footprint produced). This type of crack will always remain connected. A Palmqvist crack is produced during low indenter loading and is of a smaller scale in comparison. The Palmqvist crack will always appear in the initial stage of the crack generation during the indentation process; then, a median half-penny crack is produced once the impact of the indenter is exerted. It can be assumed that a median half-penny crack may be the result, as the ceramics are of high hardness, indicating that high indenter loads are required in order to induce visible and measurable diamond footprints.

Orange et al. [35] investigated the K_{1c} of Al_2O_3-ZrO_2 ceramic by comparing the notched beam and the Vickers indentation techniques. Cracking behaviour was observed as Palmqvist and median half-penny crack geometries were found. Low indentation loading produced Palmqvist cracks, and, with increasing loading, median half-penny cracks were found. High micro cracking was also found with the Vickers indentation technique when fine grain size (0–3 μm) ceramics were tested, and, with increasing grain size (0–5 μm), the micro cracking was reduced. With the notched-beam technique, a higher K_{1c} value was achieved with increasing grain size [35]. This means that the ceramics with larger grain boundaries have a higher K_{1c} value and higher resistance to fracture. From the work of Orange et al. [35], it can be gathered that the notched-beam indentation technique produced better results than the Vickers indentation method, although the reasons behind this were not well justified.

Median half-penny-shaped cracks occur when high indentation loads are applied [19, 32, 40]. The profile of a median half-penny-shaped crack is illustrated in Fig. 1(a). It can be predicted that the outcome for most of the crack profiles in this study would be of median half-penny shape. For cracks that are of median half-penny shape, the applicable
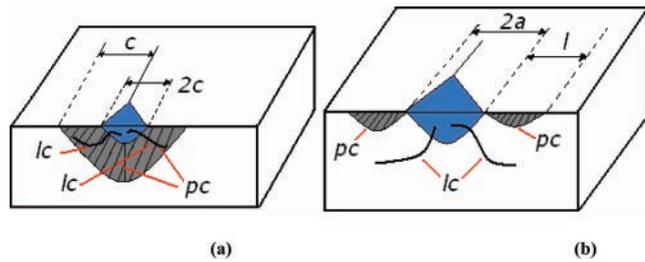
Fig. 1 Schematic diagram of (a) median half–penny crack and (b) Palmqvist crack system, where: l is the surface crack length; $2c$ or $2a$ is the length of the diamond indent; c is the centre of the diamond to the end of the crack tip; Pc is the load impact; and lc is an interior crack

equations differ (see equations (1) to (15)) [12, 13]. The indention load at which the median half-penny crack occurs for most ceramics is 3 N [19]; this was lower than the loads applied for this investigation. Therefore, it would be reasonable to assume that the generated cracks would always be of a half-penny median type crack profile. This indicated that only equations particularly applicable for median half-penny cracks should be utilized for this study in order to determine the K_{1c}. Figure 1(b) illustrates a profile of a Palmqvist crack, which tends to occur at low indentation loads [19, 40]. A Palmqvist crack is part of the median half-penny crack system because, when a load above 3 N is applied, the indenter 'pop in' occurs, and the already produced Palmqvist crack further develops into a median half-penny crack [19, 40]. These cracks are shallow and lie on the axis of the indenter, as there would be a small extension at the edge of the diamond indenter [40]. Indentation loads of up to 50 N were used for this work, and so it is likely that a Palmqvist crack will occur, leading to a half-penny median crack geometry.

4 SELECTION OF EQUATIONS FOR CALCULATING THE K_{1c}

Equations for median half-penny-shaped cracks were used for high indenter load applications. One equation was selected to calculate the K_{1c} value for the treated and as-received samples through application of the equation to the real experimental values. The equations were derived with the materials' geometrical values, which were obtained by experimental means for ceramics and glass [9, 10]. Equations (1) to (15) were mentioned in the literature to be applicable for ceramics and glass-type materials; however, no such equation was defined as applicable for a certain ceramic material type; hence, the suitability of applying the various equations to the ZrO$_2$ was not particularly defined. This is why it

was required that an investigation be carried out in order to determine the most suitable equation for this study. There were ten equations selected in this study, from various equations discussed in references [9], [10], and [17], to determine first the K_{1c} of the as-received surfaces of the ZrO$_2$ and then the laser-treated surfaces. The selected equations applicable to calculate the K_{1c}, using the Vickers indentation methods, are [9]:

$$K_{1c} = 0.0101\, P/(ac^{1/2}) \quad [38] \tag{1}$$

$$K_{1c} = 0.0515 P/c^{3/2} \quad [41] \tag{2}$$

$$K_{1c} = 0.079(P/a^{3/2})\,\log(4.5\,a/c), \\ \text{for } 0.5 \leqslant c/a < 4.5 \quad [28] \tag{3}$$

$$K_{1c} = 0.0824 P/c^{3/2} \quad [24] \tag{4}$$

$$K_{1c} = 0.4636(P/a^{3/2})(E/Hv)^{2/5}(10^{\mathrm{F}}) \quad [45] \tag{5}$$

$$K_{1c} = 0.0141(P/a^{3/2})(E/Hv)2/5 \log(8.4^{a}/c) \quad [46] \tag{6}$$

$$K_{1c} = 0.0134(E/Hv)^{1/2}(P/c^{3/2}) \quad [25] \tag{7}$$

$$K_{1c} = 0.0330(E/Hv)^{2/5}(P/c^{3/2}) \\ \text{for } c/a \geqslant \approx 2.5 \quad [28] \tag{8}$$

$$K_{1c} = 0.0363(E/Hv)^{2/5}(P/a^{1/5})(a/c)^{1.56} \quad [42] \tag{9}$$

$$K_{1c} = 0.016(E/Hv)^{1/2}(P/c^{3/2}) \quad [27] \tag{10}$$

$$K_{1c} = 0.0232\,[f(E/Hv)]P/(ac^{1/2})$$

where $F = f[\log(c/a)]$ and is determined by the data fitting

$$\text{for } c/a \leqslant \approx 2.8 \quad [47] \tag{11}$$

$$K_{1c} = 0.417\,[f(E/Hv)]P/(a^{0.42}c^{1.08})$$

where $F = f[\log(c/a)]$ and is determined by the data fitting

$$\text{for } c/a \geqslant \approx 2.8 \quad [47] \tag{12}$$

$$K_{1c} = 0.095(E/Hv)^{2/3}(P/c^{3/2}) \quad [43] \tag{13}$$

$$K_{1c} = 0.022(E/Hv)^{2/3}(P/c^{3/2}) \quad [43] \tag{14}$$

$$K_{1c} = 0.035(E/Hv)^{1/4}(P/c^{3/2}) \quad [44] \tag{15}$$

Ponton and Rawlings [10] state that the equation given by Kelly et al. [31] suggested that equation (10) has an accuracy of 30–40 per cent for ceramics that are well behaved in their indentation response. However, it is first required that the propagation of the crack geometry is understood from performing the Vickers indentation test on the as-received ZrO_2 ceramics, as further justified in this paper. It is not made clear as to why this equation was particularly used for the ceramic. It was, therefore, required that some of the relevant equations were applied to the tested values from this experiment to determine what sort of results are obtained. A hardness test was performed on the ZrO_2, assuming that the resulting cracks were of half-penny median type (as a result of applying a sufficient indentation load). Ten equations were employed, as previously stated, to establish which particular equation type produces the K_{1c} value that is the nearest to the known value for the as-received ZrO_2 ceramics, which is normally between 8 and 12 MPa m$^{1/2}$.

5 EXPERIMENTAL METHODOLOGY

5.1 Material details

The material used for the experiment was CIP ZrO_2, with 95 per cent ZrO_2 and 5 per cent yttria (Tensky International Company Ltd). Each test piece was obtained in a bulk of $10 \times 10 \times 50$ mm^3, with a surface roughness of 1.58 μm (as received from the manufacturer). This was to reduce the laser beam reflection, as the well-polished, shinier surfaces of the ceramic would reduce beam absorption. The experiments were conducted in ambient conditions at a known temperature (20 °C). All surfaces of the ZrO_2 to be treated were marked with black ink prior to the laser treatment to enhance the absorption and allow the laser beam to penetrate further into the surface.

5.2 Fibre laser treatment

A 200 W fibre laser (SPI Ltd) was used in this work, emitting a wavelength of 1.075 μm in the continuous-wave (CW) mode. Trials ranged from 75 to 150 W by varying the traverse speed for the initial experiments, to find that a traverse speed of 100 mm/min was an ideal constant to maintain for all trials, with only the laser power changing. All speeds were therefore kept to 100 mm/min for the main set of experiments presented in Fig. 2 and Table 1. Trials below 75 W for the ZrO_2 at 100 mm/min showed no evidence of any influence on the ZrO_2. Focal position was kept to 20 mm above the workpiece to obtain a 3 mm spot size for all trials. The processing gas used was compressed air at a flow rate of 25 l/min. Programming of the laser was conducted using SPI software that
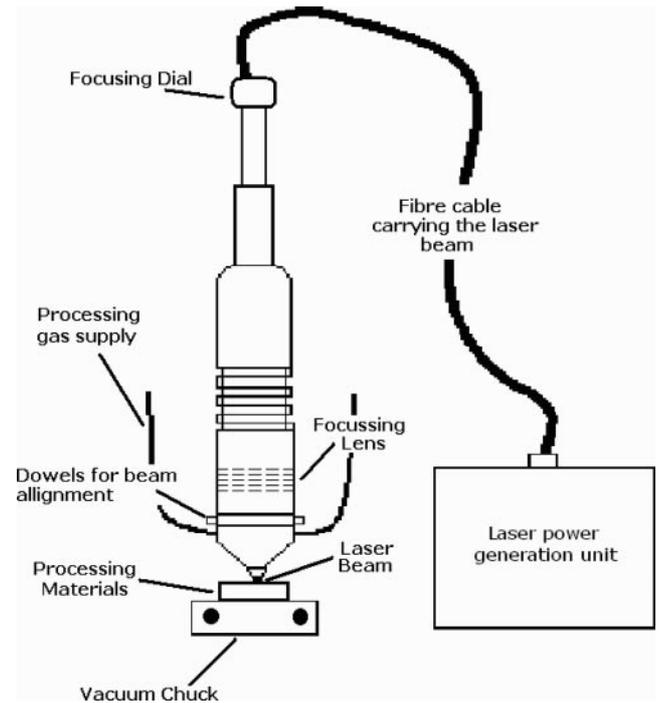

Fig. 2 Schematic diagram of the experimental set-up of the fibre laser surface treatment of the ZrO_2

Table 1 Parameters used for the fibre laser treatment of the ZrO_2

Trial no.	Power (W)	Power densities (W/mm^2)	Comments
1	75	2083.33	no visual effect
2	100	2777.77	small change in colour
3	125	4372.22	small cracks apparent
4	130	3611.11	small cracks on the edges
5	150	4166.65	large crack apparent
6	137.5	3819.44	crack-free
7	143.25	3779.16	crack-free
8	150	4166.66	apparent cracks

integrated with the laser machine. A 50 mm line was programmed using numerical control (NC) programming as a potential beam path that was transferred by .dxf file. The nozzle indicated in Fig. 2 was removed for all experiments.

5.3 Hardness indentation test and background of the Vickers indentation technique

An indenter of a specific shape, made from a diamond, was used to indent the surface of the ZrO_2 under investigation [8–19, 35, 40]. The diamond was initially pressed on to the as-received surface, and the load was then released. A diamond indentation was thus created on the surface, and its size was then measured. Thereafter, the surface area of the indentation was placed into equation (16) to calculate the hardness value:

$$Hv = 2P \sin[\theta/2]/D^2 = 1.8544P/D^2 \qquad (16)$$

where P is the load applied (kg); D is the average diagonal size of the indentation, in mm; and θ is the angle between the opposite faces of the diamond indenter, being 136° with less than ±1° of tolerance. Indentation loads of 5, 20, and 30 kg were applied. The indented surface and the resulting crack lengths were measured using the inbuilt optical microscope of the Vickers indenter (Armstrong Engineers Ltd). This method was then implemented for the surfaces of the fibre laser-treated ZrO_2. The test samples were placed under the macro indenter and were initially viewed using the built-in microscope to adjust the distance between the surface of the workpiece and the diamond indenter. This maintained a sufficient distance during each indentation and allowed a standardized testing method that complies with ISO 6507-1 [39].

5.4 Measurement of the crack lengths

Crack lengths generated by the Vickers diamond indentation test, as presented in Fig. 3(a), were measured using a contact-less, coordinate measuring machine (CMM), Flash 200. The ceramic samples were placed under a traversing lens of the optical microscope. The lens traverses in the y-direction and, to adjust the magnification, it is also able to move in the z-direction. Motion in the y-direction is provided by the bed on which the test-piece is mounted for analysis of the surface. The image appears on the screen as the optical lens traverses above the surface of the test-piece. The diamond indentations and the resulting crack lengths were measured by moving the lever in the x, y-directions and selecting a starting point on the screen where the crack ends (crack tip) and stopping on the symmetrical side of the other (symmetrical) crack tip, which produced a measurement in both the x- and y-directions.

5.5 Calculation of the fracture toughness (K_{1c})

The initial investigation used 15 equations to determine which equation type was best suited for calculating the K_{1c} [9, 10]. The as-received surfaces of the ZrO_2 were first tested for their hardness. Fifty indentations were produced on one side of the particular surface of the ZrO_2 ceramics from various test samples. Calibrated hardness was then recorded, and a mean average was measured of the as-received surfaces. Each indentation and its crack lengths were then viewed at microscopic level with the aid of the optical microscope, to observe the surface morphology. The crack lengths were measured using the Flash 200 CMM, and crack geometry was observed by a three-dimensional surface topography using white-light interferometry (Alicona Ltd, Infinite focus, IFM 2.15). The crack lengths produced by the indentations were then placed into the various K_{1c} equations with the measured average hardness. Cracking geometries were then observed in order to confirm that the cracks generated by the diamond indentation at 5 kg were of median half-penny crack profile. This ensured that equations (1) to (15) used for the median half-penny crack profile were correct. Figures 4 and 5 present an example of a typical surface profile produced from the Vickers diamond indentation using 5 kg (see Fig. 4) and 20 kg (see Fig. 5) loads. Both showed evidence of median half-penny-type crack profiles where an indenter 'pop-in', indicated in Figs 4 and 5, was exerted, and then a linear crack was produced. A Palmqvist crack profile, which tends to occur with lower indentation loads, had occurred (as indicated from the indenter 'pop-in') already in this crack geometry. The concept was more present with higher indentation loading, as presented in Fig. 5.

The equations used for this study were for half-penny median cracks. It was found that the cracks produced from the Vickers indentation test were half-penny median type, and so other equations illustrated for Palmqvist cracks were not used. Equations (1) to (10), as presented in Table 2, were used to
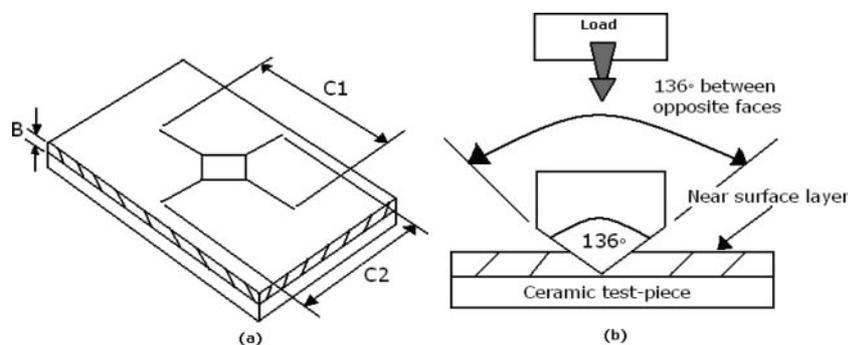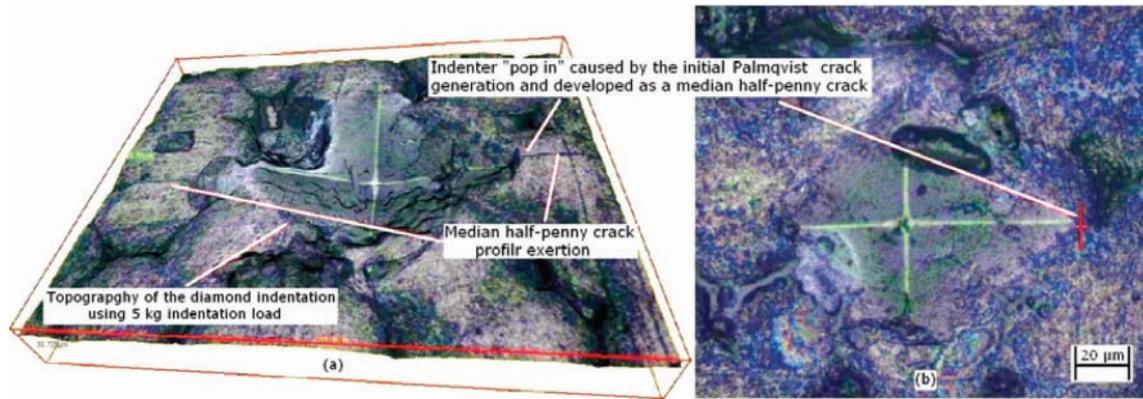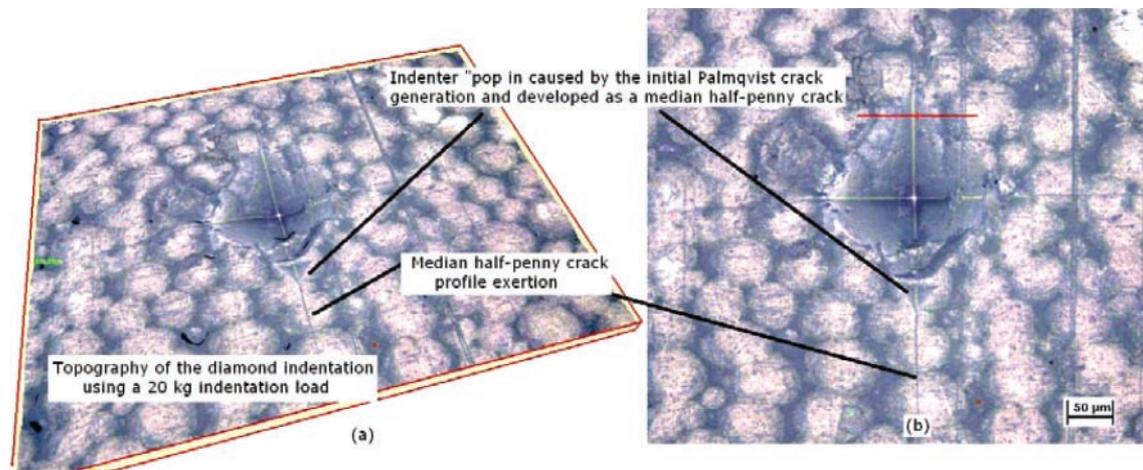

Fig. 3 Schematic diagram of a Vickers diamond indentation with (a) propagation of the cracks and (b) the concept of diamond indentation employed

Fig. 4 Topography of the Vickers diamond indentation of the as-received surface of the ZrO_2 ceramic produced by a 5 kg load, illustrating a median half-penny crack geometry

Fig. 5 Topography of the Vickers diamond indentation of the as-received surface of the ZrO_2 produced by a 20 kg load, illustrating a median half-penny crack geometry

Table 2 Ten equations used to calculate the K_{1c} for the as-received surface of the ZrO_2

Equation no.	Equation origin	Equation
1	Lawn and Swain [38]	$K_{1c} = 0.0101\ P/(ac^{1/2})$
2	Lawn and Fuller [41]	$K_{1c} = 0.0515\ P/c^{3/2}$
3	Evans and Charles [24]	$K_{1c} = 0.0824\ P/c^{3/2}$
4	Lawn et al. [25]	$K_{1c} = 0.0134\ (E/Hv)^{1/2}\ (P/c^{3/2})$
5	Niihara et al. [28]	$K_{1c} = 0.0330\ (E/Hv)^{2/5}\ (P/c^{3/2})$
6	Lankford [42]	$K_{1c} = 0.0363\ (E/Hv)^{2/5}(P/a^{1.5})$ $(a/c)^{1.56}$
7	Laugier [43]	$K_{1c} = 0.095\ (E/Hv)^{2/3}\ (P/c^{3/2})$
8	Laugier [43]	$K_{1c} = 0.022\ (E/Hv)^{2/3}\ (P/c^{3/2})$
9	Tanaka [44]	$K_{1c} = 0.035\ (E/Hv)^{1/4}\ (P/c^{3/2})$
10	Anstis et al. [27]	$K_{1c} = 0.016\ (E/Hv)^{1/2}\ (P/c^{3/2})$

Table 3 K_{1c} value obtained from ten equations for the as-received ZrO_2

Average K_{1c} (MPa m$^{1/2}$)	Percentage accuracy (K_{1c} value within range)	Status
0.90	0	Unacceptable
3.25	0	Under
5.20	0	Under
28.70	0	Unacceptable
683.64	0	Unacceptable
783.93	0	Unacceptable
2024.98	0	Unacceptable
759.60	0	Unacceptable
1208.44	0	Unacceptable
12.66	42	Acceptable

calculate the K_{1c} value for the as-received surface of the tested ZrO_2. The results have been tabulated and are presented in Table 3. The equations were set up using Microsoft Excel, which made it easy to input parameters from the full equation. These values were

hardness, crack length, Vickers indention load, and Young's modulus. It can be seen that all the values, which range between 8 and 12 MPa m$^{1/2}$ for the ZrO_2, allow the equation to be accurate and useable for calculating the K_{1c} for the laser-treated and the as-received surfaces of the ZrO_2.

P = load (kg), N = load in Newton's (N), c = average flaw size, $a = 2c$, m = length in metres, Hv = Vickers material hardness value, E = Young's modulus. (Young's modulus for all untreated samples of the ZrO_2 was kept to 210 GPa m$^{1/2}$.) For all tested samples, the indentation loads were 5 and 30 kg, and E (Young's modulus) was 210 GPa m$^{1/2}$ for the ZrO_2. The range (required for equation accuracy) is 8 to 12 MPa m$^{1/2}$ ± 0.40 MPa m$^{1/2}$. The average of the K_{1c} was obtained by using values from 50 different Vickers indentation tests. This allowed more consistency in calculating the K_{1c}, as values were used from a bigger pool of data.

The values obtained using the equations in Table 2 are presented in Table 3. The literature K_{1c} value of the untreated ZrO_2 is 8 to 12 MPa m$^{1/2}$, and so the values that do not lie in the range given for both ceramics were not considered as acceptable, and, therefore, those equations were discarded. The K_{1c} values obtained using equation (10) were reasonable for both of the materials and lie within the desired range, and so the equation was accurate and useable. Other equations were discarded and were not taken into consideration for use. Each of the equations was set up with the aid of an Excel spreadsheet. The experimental values obtained were input into the equation, such as the indentation load, crack length created by the Vickers diamond indentations, and the measured hardness. The equation that generated the most accurate result was equation (10). The Vickers diamond indenter was applied 50 times to the as-received surface plane of the ZrO_2. Hardness values from the indentation test were recorded, and the resulting crack lengths were then measured, first to calculate the K_{1c} of the untreated surface. From this, 50 K_{1c} values were obtained from one surface plane. Thereafter, an accuracy value was determined for each of the equations by taking values that were found in the range between 8 and 12 MPa m$^{1/2}$. The accuracy of the equation was determined by the number of K_{1c} values (out of 50 indentations made on one surface plane) appearing within the range between 8 and 12 MPa m$^{1/2}$. The K_{1c} values within this range were considered as accurate and were used to calculate the accuracy of the equations. Up to 42 per cent accuracy was found using the same equation with the as-received surface of the ZrO_2. Other equations applied were discarded as they proved to be of minimal use owing to their results from this investigation. Values obtained using equation (10) were most accurate (closer to the required range for the ZrO_2) in comparison with the other equations; consequently, this equation was used for all as-received and laser-treated surfaces of the ZrO_2 to determine the K_{1c}.

The ceramic surfaces were first treated with the fibre laser. The K_{1c} values were then calculated using equation (10). The reason for changing the Young's modulus from 210 GPa to 260 GPa for the ZrO_2 was because of the ceramics being anisotropic (meaning the Young's modulus of the material was not uniform around all orientations of the material). This may occur owing to certain manufacturing impurities and further modifications having occurred during processing of the ceramic. As the ceramic was exposed to the fibre laser beam (thermal energy), this led to the induction of further changes within the material from the induced thermal stress, indicating that the Young's modulus value for all laser-treated samples would ideally be increased when the K_{1c} was calculated. This is why the Young's modulus was changed for the fibre laser-treated samples when determining the K_{1c} of the ZrO_2 engineering ceramic.

6 RESULTS AND DISCUSSION

6.1 Analysis of the as-received surfaces: using a 30 kg indentation load

The average surface hardness of the as-received surface was found to be 1141 Hv for ZrO_2 (see Fig. 6 and Table 4). The values provided by the manufacturer for the as-received surfaces were 800 to 1200 Hv for ZrO_2. The ceramics were manufactured using the CIP method, which may have left porosity and surface flaws in the ZrO_2 in comparison with hot isostatic pressing (HIP). The highest value was 1129 Hv, and the lowest was 757 Hv, when an indentation load of 30 kg was applied. This fluctuation has occurred owing to several factors such as: porous structure; the ceramic's response to the diamond indentation; surface flaws and micro cracks pre-existing on the ceramic, operator; and machine accuracy in measuring the sizes and footprints of the diamond indentations. Operator accuracy depends purely on the ability of the operator to locate and measure the size of the diamond footprint through the inbuilt lens of the Vickers indentation machine. Such errors were minimized in the work herein, as the diamond footprints and the resulting crack lengths were both measured using computational means. However, the machine accuracy of 875 nm for a load of 5 kg and 1471.5 nm for a load of 30 kg must be taken into consideration when conducting the Vickers indentation test [48].

The fluctuation found in the mean hardness from the results of this study was up to 11 per cent. This, in comparison with the values for ZrO_2 given in the literature, was 1 per cent higher than the ± 10 per cent range (error) given in [13]. An error of 1 per cent between the hardness values found in this study and the literature can be excepted from being a non-conformance and may be considered to pass the
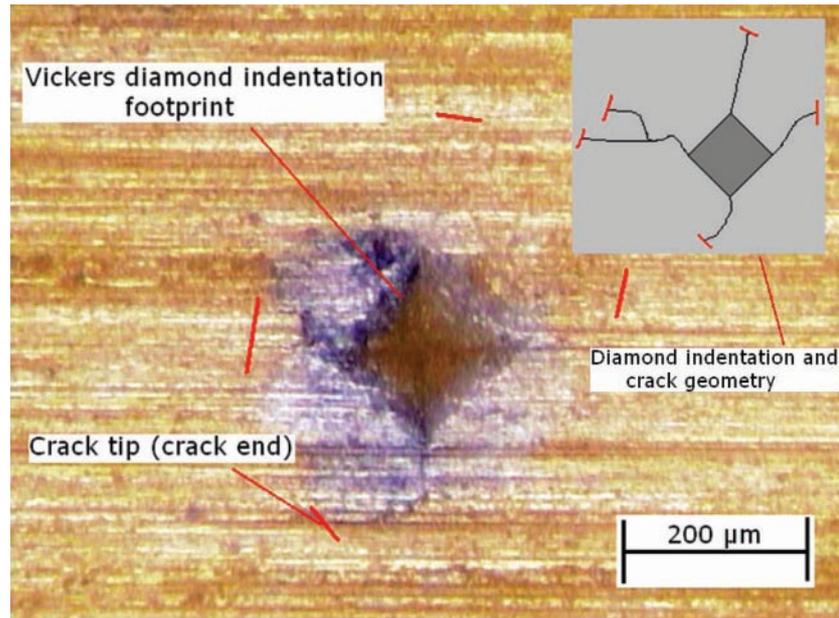
Fig. 6 Example of the as-received surface of ZrO_2 indented by a 30 kg load (hardness $= 926$ Hv; crack length $= 437$ μm; $K_{1c} = 6.94$ MPa m$^{1/2}$)

Table 4 Summary of the results illustrating an increase or decrease in the parameters used for calculating the K_{1c} of the as-received and laser-treated surface of the ZrO_2 ceramics

	Average surface hardness, Hv		Average surface crack length (μm)		Average surface K_{1c} (MPa m$^{1/2}$)	
As-received surface using 5 kg load	983	0	277	0	2.48	0
Fibre laser-treated surface	940	4% lower	177	38% lower	5.62	56% increase

Note: Values for the fibre laser-treated surface were compared with the values of the as-received surface indented using a 5 kg load to determine the percentage rise and decrease

quality requirements if the hardness test was used for a (real-life) ZrO_2 ceramic engineering component/product.

The average crack length produced from the Vickers indentation test was 276 μm for the ZrO_2. Results from 50 indentations present crack lengths that range from 221 μm as the lowest to 335 μm as the highest. The variation from its mean value was wide owing to the micro cracks pre-existing on the ZrO_2's surface. If the surface were well polished, the results of the crack lengths would be much lower, as the surface would be less prone to cracking after grinding and fine polishing of the ZrO_2. However, a smoother surface would prevent the laser from being absorbed sufficiently into the material surface and often has the tendency to reflect more than absorb, and so the surfaces were not polished and were tested as received from the manufacturer.

From applying a 30 kg load, it was found that the cracks were significantly large owing to the amount of force acting on the surface area of the ZrO_2. An

example of such a crack profile is shown in Fig. 6. It was therefore interesting to investigate the crack lengths produced with a lower indentation load, which predictably would have a smaller effect on the end value of the K_{1c} of the ZrO_2 engineering ceramic. As such, a 5 kg indentation load was used: owing to the force over the surface area being much lower, it produced a smaller footprint of the diamond and smaller crack lengths. This would, therefore, result in producing a lower K_{1c} value than in the literature and the manufacturer's range given for the ZrO_2.

The K_{1c} values for the as-received surfaces after application of an indentation load of 30 kg, as presented in Fig. 7, show that the values obtained complied with the values given in the literature and the values given by the manufacturer [1, 13]. The average K_{1c} for the ZrO_2 was found to be 12.7 MPa m$^{1/2}$. The graph in Fig. 7 indicates that there is a significant level of fluctuation for the values above and below the mean range.

The highest value above the mean was found to be 18.11 MPa m$^{1/2}$, and the lowest value below the mean was 8.52 MPa m$^{1/2}$. This has occurred owing to the following factors:

1. A change in the material hardness influences the end K_{1c} value. A change in hardness of ± 100 Hv resulted in a change in the final K_{1c} value of ± 0.34 MPa m$^{1/2}$ (according to equation (10)).
2. A change in the crack length (being the major parameter in equation (10), as used in this work) by ± 100 μm resulted in a change in the end K_{1c} value of ± 6.31 MPa m$^{1/2}$, if the hardness was up to 1250 Hv as a particular input parameter in the calculation. Hence, the crack length has a bigger influence on the K_{1c} value than the hardness.
3. The surface micro cracks and porosity pre-existing on the ZrO$_2$ surface make it prone to cracking and reduce the ceramic's resistance to fracture.
4. The response of the ZrO$_2$ to diamond indentation in some of the areas within the ZrO$_2$ produced fluctuating values as opposed to other areas from the viewpoint of the crack length, porosity, and the surface flaws.

The surface condition should also be considered, as the surface roughness for the ZrO$_2$ was exceptionally high for conducting the Vickers indentation test, and this would have resulted in producing higher crack lengths that further resulted in a reduction in the ZrO$_2$'s K_{1c} value.

6.2 Analysis of the as-received surfaces: using a 5 kg indentation load

The hardness of the ZrO$_2$ obtained after applying a 5 kg load was much lower than the hardness values obtained after applying a load of 30 kg. This was because the 5 kg load applied to the material's surface area resulted in lower penetration of the diamond indentation into the ZrO$_2$, as well as the surface area of the diamond footprint being smaller in dimension, which resulted in the generation of a lower hardness value. The average hardness value for the ZrO$_2$ was 983 Hv, with the highest value being 1330 Hv above the mean and the lowest being 707 Hv below the mean. The hardness values of the ZrO$_2$ using a 5 kg load agree with the hardness values provided by the manufacturer; however, they were found to be towards a bottom limit. A possible cause of this vast fluctuation in the values may have been the ZrO$_2$ exhibiting micro cracks, porosity, and impurities on the near surface layer in comparison with the bulk hardness, which frequently produced non-uniform results.

The results showed minimal difference in the generated crack lengths for the ZrO$_2$ obtained by applying a 5 kg load in comparison with the results obtained by applying a 30 kg load. The average crack length was 279 μm. Despite the indentation load and the applied force being much smaller in comparison with the 30 kg load, the material was still cracking in equivalent measure to the results of the trials conducted using a higher load. This clearly indicated that the surface did not exhibit a good response during the indentation test. This meant that a smoother surface finish was required for the indentation test in order to overcome this problem, so that the surface scarring and micro cracks pre-existing on the ZrO$_2$ were minimized, and the strength of the top surface layer is further enhanced for a better indentation response. This also has the possibility of increasing the surface hardness and yet, at the same time, would reduce the resulting cracks from the Vickers diamond footprints and avoid crack bridging between the
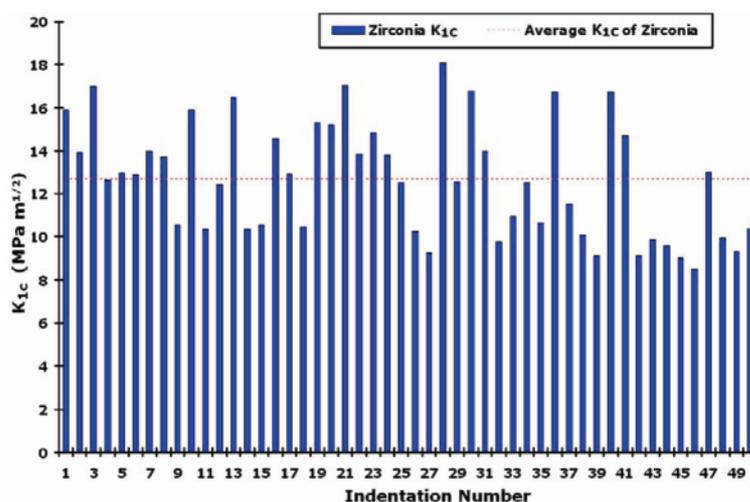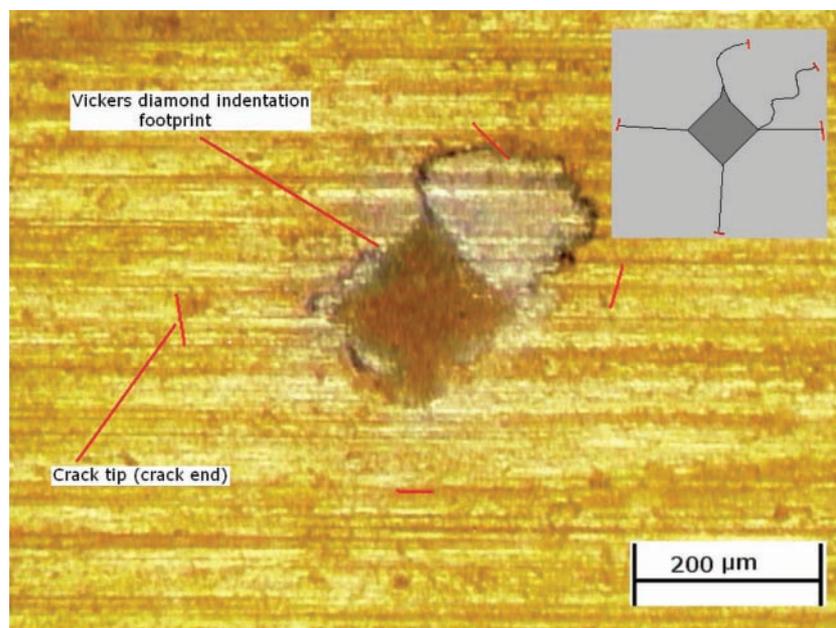

Fig. 7 K_{1c} of the as-received surface of the ZrO$_2$ after application of a 30 kg load

diamond footprints and the pre-existing surface micro cracks.

Ponton and Rawlings [9] suggested that a minimum loading of 50 N must be pressed in order to produce a diamond indentation; the minimum loading used herein agrees with the work of Ponton and Rawlings [9]. However, the loading herein was 49.05 N, and we still see a diamond indentation, as presented in Fig. 8, with a median half-penny-shape profile. Initial experiments using lower indentation loads such as 24.5 N and 9.8 N also presented a sufficient indented footprint from the Vickers hardness test. The diamond indentation in Fig. 8 is smaller in size than the indentation created by the 30 kg load.

However, the average crack lengths found using a 5 kg indentation load were of equal size to those found with the 30 kg load. The difference between the average values for the two test results was 3 per cent and less when considering a larger pool of data. From this, it can be gathered that the macro hardness indentation test may be more stable at higher indentation loads than lower, particularly with hard, brittle materials such as ZrO_2.

The results found for hardness herein when employing a 30 kg indentation load match the values provided by the manufacturer and prove that the method used for the hardness calculation and measurement of the crack lengths was valid, although the

Fig. 8 Example of the as-received surface of ZrO_2 indented by a 5 kg load (hardness $= 1120$ Hv; crack length $= 425\,\mu m$; $K_{1c} = 1.10\,MPa\,m^{1/2}$)
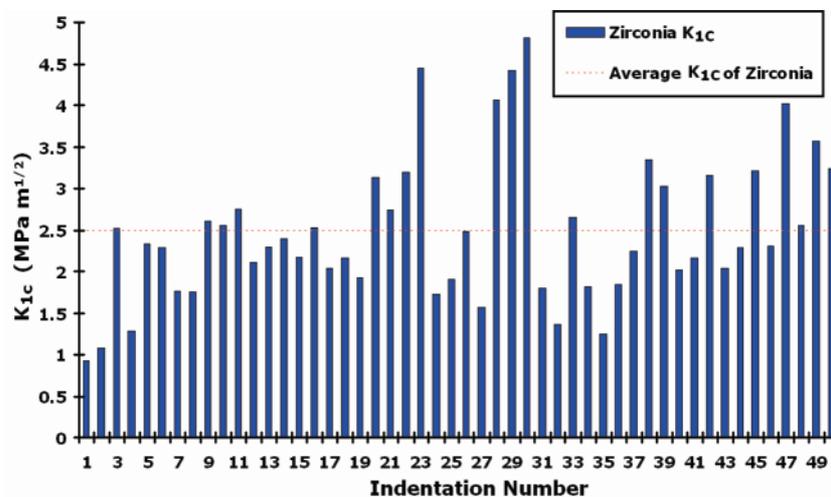
Fig. 9 K_{1c} of the as-received surfaces of the ZrO_2 after application of a 5 kg indentation load

values for the hardness are much smaller than the values provided in the manufacturer's specification when a 5 kg load was used. This was owing to the fact that the indentation load was much smaller and produced smaller footprints of the diamond, which exerted lower force on the surface and reduced the end value of the K_{1c}. The average K_{1c} was found to be 2.53 MPa m$^{1/2}$ for the ZrO$_2$, as presented in Fig. 9, which also shows the highest value to be 6.02 MPa m$^{1/2}$ and the lowest to be 0.88 MPa m$^{1/2}$. The hardness could be much higher if the surfaces were ground and polished prior to the Vickers indentation test, as previously stated. This would minimize the surface micro cracks and result in better consistency in achieving the hardness value and the resulting crack lengths. The surfaces were tested as received owing to the comparison made with the laser-treated surface, as the ground and polished surfaces would enhance the material's reflectivity of the laser beam and would minimize the laser beam absorption into the ZrO$_2$; consequently, a compromise was required to be made.

6.3 Analysis of the fibre laser-treated surfaces: using a 5 kg indentation load

The mean hardness found was 940 Hv on the fibre laser-treated ZrO$_2$ surface. The highest value above the mean was 1089 Hv, and the lowest was 826 Hv. There was a 4.5 per cent difference between the average hardness values obtained from the fibre laser treatment and those obtained from the as-received surface. The fibre laser had decreased the hardness in comparison with that of the as-received surface of the ZrO$_2$. The average crack length of the fibre-treated ZrO$_2$ was 171 μm. The crack length was much reduced in comparison with the crack length of the

as-received surface, which was 277 μm. The fibre laser-treated surfaces also had much smaller cracks in comparison with the as-received surface (see example in Fig. 10). The reduction in the surface hardness indicated that the laser surface treatment had softened the top (near) surface layer of the ZrO$_2$. From this, it can be assumed that some degree of melting and solidification may have taken place during the laser–ceramic interaction. This would have caused a localized ductile surface to have formed, along with a change in the surface composition. Further studies are being undertaken to determine this effect.

The average K_{1c} value for the ZrO$_2$ after the fibre laser treatment was 5.62 MPa m$^{1/2}$. The highest K_{1c}
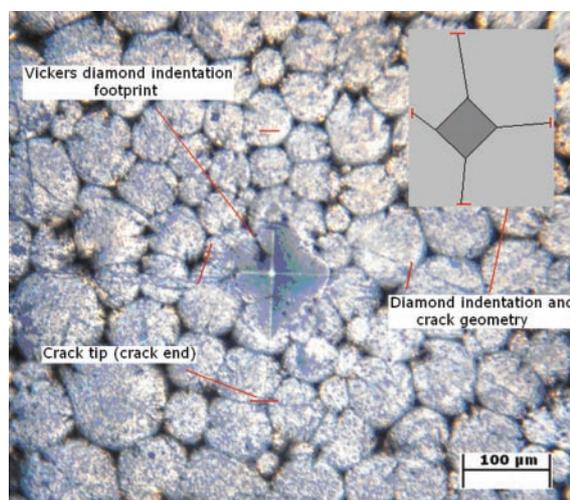

Fig. 10 Example of the fibre laser-treated surface of the ZrO$_2$ indented by a 5 kg load, laser power = 150 W, 100 mm/min, 3 mm post size (hardness = 654 Hv; crack length = 232 μm; K_{1c} = 3.97 MPa m$^{1/2}$)
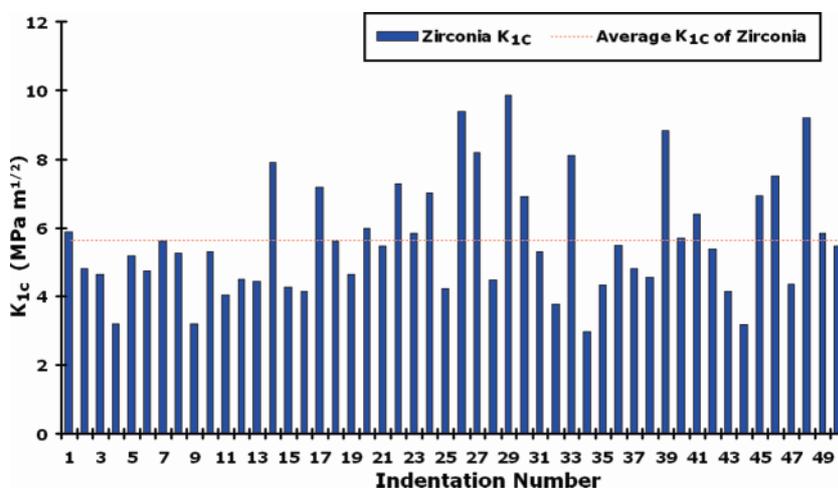

Fig. 11 K_{1c} of the fibre laser-treated surfaces of ZrO$_2$ after application of 5 kg indentation load

value obtained above the mean was 9.85 MPa m$^{1/2}$. The lowest value below the mean was 2.97 MPa m$^{1/2}$ for the ZrO$_2$, as presented in Fig. 11 and Table 4. The K_{1c} values for the fibre laser-treated ZrO$_2$ surface were enhanced by 56 per cent in comparison with those of the as-received surfaces. The values in Fig. 11 fluctuate owing to the softening of the treated surface, which would have generated lower cracks during the indentation test. Those areas where K_{1c} is high indicate that the localized, near-surface layer has more resistance to crack propagation under cyclic loads or during the onset of any tensile stresses. The Young's modulus is another factor that also influenced this change in the ZrO$_2$'s K_{1c}. The Young's modulus was increased from 210 GPa (as-received surface) to 260 GPa (laser-treated surface) when the K_{1c} was being determined. This was because the ratio of stress and strain was higher after the laser treatment. Owing to the way in which the Young's modulus contributing to the K_{1c} equation was used, it was likely that the influence of the Young's modulus was significant in calculating the K_{1c} values in this investigation. The end value of the K_{1c} would be slightly reduced during the calculation of the K_{1c} of the laser-treated ZrO$_2$ in the case of the Young's modulus being kept the same for the as-received surface.

7 CONCLUSIONS

Empirical equations were used on the as-received surfaces of the ZrO$_2$ to investigate the most suitable equation for calculating the K_{1c}. Palmqvist cracks were produced, leading to half-penny median type cracks observed from the topographical investigation at indentation loads of 5, 20, and 30 kg. This confirmed the use of the group of equations applied for the investigation. The results from the computational analysis showed that equation (10) ($K_{1c} = 0.016$ $(E/Hv)^{1/2}(P/c^{3/2})$) by Anstis et al. [27] was the most accurate. It produced 42 per cent accuracy with the K_{1c} values that were found within the range (8 to 12 MPa m$^{1/2}$) given in the literature and by the manufacturer of the ZrO$_2$.

The as-received surface analysis showed that the most influential parameter in calculating the K_{1c} was crack length, as it proved that longer cracks produced by the Vickers indentation led to lower resistance for the ZrO$_2$ to propagate a crack. Surfaces with shorter crack lengths exhibited higher resistance to indentation, which further led to an improved K_{1c} value. Hardness also influenced the ZrO$_2$'s K_{1c}, as the results showed that surfaces with high hardness produced bigger crack lengths, which reduced the K_{1c}, and lower surface hardness reduced the crack propagation. This complied with the concept of softer (ductile) surfaces being less prone to cracking.

Furthermore, the changes in the hardness demonstrated that the hardness acted as an influential parameter in changing the surface K_{1c} value of the ZrO$_2$. The average hardness of the as-received surface was found to be 983 Hv, with the average crack length being 277 μm using a 5 kg indentation load, which led to an average surface K_{1c} value of 2.48 MPa m$^{1/2}$.

It was found that higher indentation loads produced bigger diamond footprints and generated greater crack lengths. However, the K_{1c} values were also increased with the higher load, owing to the indentation load also being an important function of the K_{1c} equation when the indentation method is employed to determine the ceramic's K_{1c}. The increase in the Young's modulus had affected the K_{1c} value, owing to the ratio of stress to strain possibly increasing after the laser treatment. The values of K_{1c} for the fibre laser-treated surface would be slightly lower if stress and strain were not considered.

Comparison of the as-received surface with the fibre laser-treated surface, as presented in Table 4, showed improvement in the K_{1c} value of the top (near) surface layer of the fibre laser-treated ZrO$_2$. The hardness was reduced by 4 per cent, which resulted in lowering of the crack lengths to 38 per cent. The average hardness found with the fibre laser-treated surface was 941 Hv, with the average crack length being 177 μm. This resulted in boosting the K_{1c} value to 5.62 MPa m$^{1/2}$, which was 56 per cent higher in comparison with the as-received surface. This was owing to the hardness and the crack lengths produced by the Vickers indentation being lower than those of the as-received surface. From this, it was indicative that the laser treatment had softened the localized surface layer as the surface melted and solidified. Further investigations are being undertaken to elaborate this effect.

Despite the advantages, the Vickers indentation method to calculate the ceramic's K_{1c} in general comprises of many flaws, such as the results obtained from the hardness test heavily depending on the operator's ability to detect the crack lengths and the geometry. Also the ceramics geometrical response to the diamond indentation as well as the level of surface roughness of the ceramic, since a smoother surface than the used in this study would result in a higher surface strength and in fluence the hardness and the resulting crack length values. The K_{1c} results could be much more accurate if a consistent surface hardness value was obtained, along with its crack geometry, which could be found from employing other indentation techniques as well as various other methods using many other existing equations, which would also produce variation in the K_{1c} value.

© Authors 2010

REFERENCES

1 **Richardson, D.** *Modern ceramic engineering*, third edition, 2006 (CRC Press, Taylor & Francis Group).

2 **Kawamura, H.** New perspectives in engine applications of engineering ceramics. *Science of Engineering Ceramics II*, International Symposium, 1999, vol. 161, pp. 9–16.

3 **Mikijelj, B.** and **Mangels, J.** SRBSN material development for automotive applications. Seventh International Symposium on *Ceramic Materials and Components for Engines*, 2000.

4 **Mikijelj, B., Mangels, J.,** and **Belfield, E.** High contact stress applications of silicon nitride in modern diesel engines. Institution of Mechanical Engineers, *Fuel Injection System Conference*, London, 2002.

5 **Mangels, J.** A proven ceramic material for engine applications. Institution of Mechanical Engineers, *Fuel Injection System Conference*, London, 2006.

6 **Spriggs, R. M.** Applications and prospective markets for advanced technical ceramics. *Key Applications of Materials*, 1999, **56–57**, 1–12.

7 **Rödel, J., Kounga, A. N., Weissenberger-Eibl, M., Koch, D., Bierwisch, A., Rossner, W., Hoffmann, M., Danzer, R.,** and **Schweider, G.** Development of a road map for advanced ceramics: 2010–2025. *J. European Ceramic Soc.*, 2009, **29**, 1549–1560.

8 **Shukla, P. P.** *Laser surface treatment of silicon nitride using contact-less energy beams*, MSc by Research thesis, Coventry University, United Kingdom, 2007.

9 **Ponton, C. B.** and **Rawlings, R. D.** Vickers indentation fracture toughness test, Part 1 – Review of literature and formulation of standardised indentation toughness equations. *Mater. Sci. Technol.*, 1989, **5**, 865–872.

10 **Ponton, C. B.** and **Rawlings, R. D.** Vickers indentation fracture toughness test, Part 2 – Review of literature and formulation of standardised indentation toughness equations. *Mater. Sci. Technol.*, 1989, **5**, 961–976.

11 **McColm, I. J.** *Ceramic hardness*, 1990, (UK, University of Bradford, New York, Platinum Press).

12 **Mitcjell, T. E.** Dislocations in ceramics. *Mater. Sci. Technol.*, 1985, **1**, 944–949.

13 **Castaing, J.** and **Veyssiere, P.** Core structure dislocations in ceramics. Crystal lattice defects and amorphous materials. 1985, **12**, 213–227.

14 **Rabier, J.** Plastic deformation and dislocations in ceramic materials. *Radiation Effects and Defects in Solids*. 1995, **137**, 205–212.

15 **Mohanty, P. S.** and **Mazumder, J.** Solidification and microstructural evolution during laser beam- material interaction. *Metall. Mater. Trans. B*, 1998, **29B**, 1269–1279.

16 **Ahn, Y., Chandrasekar, S.,** and **Farris, T. N.** Determination of surface residual stress in machined ceramics using indentation fracture. *J. Mfg Sci. Engng*, 1996, **118**, 483–489.

17 **Liang, K. M., Orange, G.,** and **Fantozzi, G.** Evaluation by indentation of fracture toughness of ceramics. *J. Mater. Sci.*, 1990, **25**, 207–214.

18 **Chicot, D.** New development for fracture toughness determination by Vickers indentation. *Mater. Sci. Technol.*, 2004, **20**, 877–884.

19 **Matsumoto, R. K. L.** Evaluation of fracture toughness determination method as applied to ceria – stabilized tetragonal Zirconia polycrystal. *J. Am. Ceram. Soc.*, 1987, **70**, 366–368.

20 **Liang, K. M., Orange, G.,** and **Fantozzi, G.** Crack resistance and fracture toughness of Alumina and Zirconia ceramics: Comparison of notched- beam and indentation technique. Science Ceramics 14th International Conference1988, **14**, pp. 709–714.

21 **Exner, H. E.** The influence of sample preparation on Palmqvist's method for toughness testing of cemented carbides. *Trans. Metall. Soc. AIME*, 1989, **245**(4), 677–683.

22 **Marion, R. H.** In fracture mechanics applied to brittle materials. STP 678 (Ed. S. W Freiman), 1979, pp. 103–111 (ASTM , Philadelphia, PA).

23 **Evans, A. G.** and **Wilshaw, T. R.** Quasi static particle damage in brittle solids. *Acta Metall.*, 1976, **24**, 939–956.

24 **Evans, A. G.** and **Charles, E. A.** Fracture toughness determinations by indentation. *J. Am. Soc.*, 1976, **59**(7–8), 371–372.

25 **Lawn, B. R., Evans, A. G.,** and **Marshall, D. B.** Elastic/ plastic indentation damage in ceramic: the median/ radial crack system. *J. Am. Ceram. Soc.*, 1980, **63**(9–10), 574–581.

26 **Marshall, D. B.** Failure from contact induced surface flaws. *J. Am. Ceram. Soc.*, 1983, **66**, 127–131.

27 **Anstis, G. R., Chanrikul, P., Lawn, B. R.,** and **Marshall, D. B.** J. Am. Ceram. Soc.. 1981, **64**, 533–538.

28 **Niihara, K., Morena, R.,** and **Hasselman.** Evaluation of K_{1c} of brittle solids by the indentation method with low crack-to-indent ratios. *J. Mater. Sci. Lit.*, 1982, **1**, 13–16.

29 **Tani, T., Miyamoto, Y.,** and **Koizumi, M.** Grain size dependences of Vickers microhardness and fracture toughness in Al_2O_3 and Y_2O_3 ceramics. *Ceram. Int.*, 1986, **12**(1), 33–37.

30 **Hoshide, T.** Grain fracture model and its application to strength evaluation in engineering ceramics. *Engng Fracture Mech.*, 1993, **44**(3), 403–408.

31 **Kelly, J. R., Cohen, M. E.,** and **Tesk, J. A.** Error biases in the calculation of indentation fracture toughness for ceramics. *J. Am. Ceram. Soc.*, 1993, **76**(10), 2665–2668.

32 **Li, Z., Gosh, A., Kobayashi, A. S.,** and **Bradt, R. C.** Indentation fracture toughness of sintered silicon nitride in the Palmqvist crack regime. *J. Am. Ceram. Soc.*, 1989, **72**, 904–911.

33 **Strakna, T. J.** and **Jahanmir, S.** Influence of grinding direction on Fracture strength of silicon nitride. *Machining Adv. Mater.*, 1995, **208**, 53–64.

34 **Gong, J.** Determining indentation toughness by incorporating true hardness into fracture mechanics equations. *J. Eur. Ceram. Soc.*, 1998, **19**, 1585–1592.

35 **Orange, O., Liang, K. M.,** and **Fantozzi, G.** Crack resistance and fracture toughness of alumina and Zirconia ceramics: comparison of notched beam and indentation technique. *Sci. Ceram.*, 1987, **14**(7–9), 709–714.

36 Glandous, J. C., Rouxl, T., and **Qiu, T.** Study of the Y-TZP toughness by an indentation method. *Ceram. Int.*, 1991, **17**, 129–135.

37 Fischer, H., Waindich, A., and **Telle, R.** Influence of preparation of ceramic SEVNB specimens on fracture toughness testing results. *Dental Mater.*, 2006, **24**, 618–622.

38 Lawn, B. R. and **Swain, M. V.** Microfracture: beneath point indentations in brittle solids. *J. Mater. Sci.*, 1975, **10**, 113–122.

39 British Standards. Vickers hardness test – Part 2 – Verification and calibration of testing machines, 2005, Metallic Materials – ISO 6507-1.

40 Lawn, B. R. and **Wilshaw, T. R.** Indentation fracture: principles and application. *J. Mater. Sci.*, 1975, **10**, 1049–1081.

41 Lawn, B. R. and **Fuller, E. R.** Equilibrium penny-like cracks in indentation fracture. *J. Mater. Sci.*, 1975, **10**, 2016–2024.

42 Lankford, J. Indentation microfracture in the Palmqvist crack regime: implication for fracture toughness evaluation by the indentation method. *J. Mater. Sci. Lett.*, 1982, **1**, 493–495.

43 Laugier, M. T. The elastic/plastic indentation of ceramics. *J. Mater. Sci. Lett.*, 1985, **4**, 1539–1541.

44 Tanaka, K. Elastic/plastic indentation hardness and indentation fracture toughness: The inclusion core model. *J. Mater. Sci.*, 1987, **22**, 1501–1508.

45 Evans, A. G. Fracture mechanics applied to brittle materials. STP 678 (Ed. S. W. Freiman), 1979, pp. 112–135 (ASTM,Philadelphia, PA).

46 Blendell, J. E. PhD thesis, Massachusetts Institute of Technology, 1979.

47 Miranzo, P. and **Moya, J. S.** Elastic/plastic indentation in ceramics: a fracture toughness determination. *Ceram. Int.*, 1984, **10**(4), 147–152.

48 Ullner, C., Reimann, E., Kohlhoff, H., and **Subaric-Leitis, A.** Effect and measurement of the machine compliance in the macro range of instrumented indentation test. *Measurement*, 2010, **43**, 216–222.

APPENDIX

Notation

a	Twice the average flaw size ($2c$)
c	Average flaw size
D	Average diagonal size
E	Young's modulus
F	$f[\log (c/a)]$
Hv	Hardness
K_{1c}	Fracture toughness
NC	Numerical control
P	Load (Kg)
Pc	Load impact